



Electromagnetic field generated by a wireless energy transfer system: comparison of simulation to measurement

E. N. Baikova, L. Romba, S. S. Valtchev, R. Melicio, V. Fernão Pires, A. Krusteva & G. Gigov

To cite this article: E. N. Baikova, L. Romba, S. S. Valtchev, R. Melicio, V. Fernão Pires, A. Krusteva & G. Gigov (2018) Electromagnetic field generated by a wireless energy transfer system: comparison of simulation to measurement, Journal of Electromagnetic Waves and Applications, 32:5, 554-571, DOI: [10.1080/09205071.2017.1399832](https://doi.org/10.1080/09205071.2017.1399832)

To link to this article: <https://doi.org/10.1080/09205071.2017.1399832>



Published online: 08 Nov 2017.



Submit your article to this journal [↗](#)



Article views: 67





View related articles [↗](#)



View Crossmark data [↗](#)



Electromagnetic field generated by a wireless energy transfer system: comparison of simulation to measurement

E. N. Baikova^{a,b}, L. Romba^a, S. S. Valtchev^a, R. Melicio^{c,d} , V. Fernão Pires^{e,b} ,
A. Krusteva^f and G. Gigov^g

^aFaculdade de Ciências e Tecnologia, UNINOVA-CTS, Universidade Nova de Lisboa, Lisbon, Portugal;

^bDepartamento de Engenharia Eletrotécnica, Escola Superior de Tecnologia, Instituto Politécnico de Setúbal, Setúbal, Portugal; ^cIDMEC, Instituto Superior Técnico, Universidade de Lisboa, Lisbon, Portugal;

^dDepartamento de Física, Escola de Ciências e Tecnologia, Universidade de Évora, Évora, Portugal; ^eINESC-ID, Instituto de Engenharia de Sistemas e Computadores, Lisbon, Portugal; ^fResearch & Development Sector, Technical University of Sofia Sofia, Bulgaria; ^gPower Electronics Department, Technical University of Sofia, Sofia, Bulgaria

ABSTRACT

This paper presents a wireless energy transfer system operating at the frequency values of kHz order: modeling, simulation, and comparison with prototype measurement results. Wireless energy transfer system model using finite element method was carried out to simulate the electric field and the magnetic flux density for different air gap sizes between the transmitter and the receiver coils. Results are presented and compared with the electromagnetic emission measurements radiated by the wireless energy transfer system prototype. The electric field comparison between the simulated and the prototype measurement values shows an error of roughly 8.7%. In the recent years, the interest in the wireless energy transfer technology, especially for electric vehicles batteries charging, is rapidly increasing. As a result of the increasing application of this technology in the industrial and consumer electronic products, more concerns are raised about the electromagnetic compatibility, since the wireless energy transfer systems produce electromagnetic emissions in the surrounding environment.

ARTICLE HISTORY

Received 12 July 2017

Accepted 24 October 2017

KEYWORDS

Wireless energy transfer; electric field; magnetic flux density; modeling; simulation; prototype

1. Introduction

The wireless energy transfer (WET) system for charging of electronic equipment batteries is in the same time, a source of radiated electromagnetic energy that is injected into the surrounding environment. In the case of consumer electronic equipment, the applied power is in the order of tens of Watts. In comparison, the commercial equipment for contactless electric vehicles charging, applies power level in the order of several kW. Thus, it is more likely that the increased level of radiated electromagnetic energy in this last case could adversely affect humans and other biological organisms.

The electromagnetic compatibility (EMC) treats from the WET system increases the need of a detailed analysis of the electromagnetic (EM) processes in the human body exposed to radiated electromagnetic energy. Moreover, it is very important to take steps to mitigate the electromagnetic field levels produced by a WET system. Thus, the researchers should know about standards and regulations, such as exposure limits for electromagnetic fields, specific absorption rates in the human body, and monitor the development of new regulations. On the other hand, the standardization and regulatory bodies should be informed of research efforts in this area, especially on issues of preferred spectrum bands, potential interference with other wireless communication systems, and radiological safety studies. There is necessity to diffuse knowledge to regulators and back into researchers [1].

The stray EM field emitted by WET systems is highly non-uniform and may exceed the reference levels established already by the international guidelines [2]. The study of the electromagnetic influence on the human health is important not only for its easily measurable short-term consequences. The long-term consequences from the exposure of humans and other biological objects to the radiation is also studied [3].

According to the ICNIRP Guidelines [4], the electric field limits, for the general public exposure in the frequency range of 3 kHz to 1 MHz, is $E = 87 \text{ V/m}$, as shown in the Figure 1. For the occupational public, the exposure limits are less restrictive and for the same frequency band, the limit is $E = 610 \text{ V/m}$. This difference is explained by the fact that the occupational public is considered to consist of healthy adults, aware of the risks, and exposed only during working periods of time. In turn, the general public represents the large diversity of health sensitivities and is potentially exposed 24 h daily, unconscious of the risks.

Considering that the 'in vivo' study of the electromagnetic field distribution in the human body will be impossible, the only opportunity to evaluate the impact of the EM field on the living beings is by modeling and simulation. Recently, some articles were published, discussing the modeling and simulation of the electromagnetic process in wireless energy transfer systems.

In [5–13], the circuit parameters of the wireless energy transfer system are obtained by calculation based on the finite element method (FEM). Subsequently, a computational model of the WET system is built, based on the parameters obtained from the analysis. The

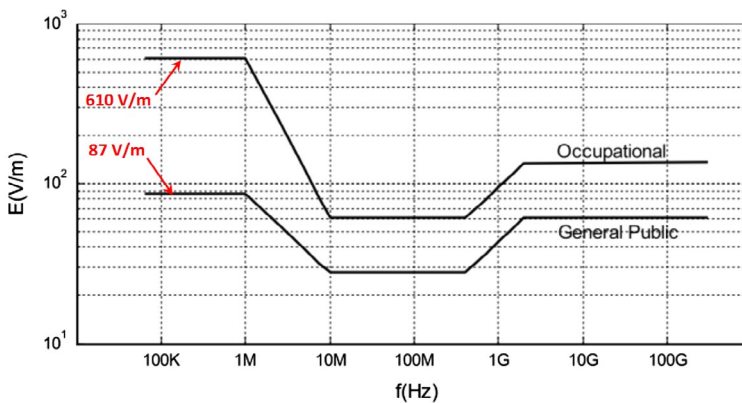


Figure 1. Electric field exposure limits by ICNIRP.

characteristics, i.e. the power loss, equivalent circuit values, magnetic and electric field intensity, the efficiency of the system are observed in a software simulation.

A WET system with magnetically coupled resonators is presented in [5]. The system is modeled and calculated applying the FEM analysis. In this publication, the influence of the applying of a 'met' material, known as perfect magnetic conductor, on the efficiency of the WET system is simulated and presented.

In [6], the model for the wireless energy transfer research is studied, at the example of inductively-coupled coils of irregular shape. The circuit parameters, such as inductance, coil resistance, and self-capacitance are defined through electromagnetic energy assessment, made by the finite element method. Spatial distribution of the current per unit and spatial distribution of the vector of the magnetic potential for different air gaps between the coils, are presented.

A modeling of inductive energy transfer coils in the frequency domain, using the FEM tools and Ansys Maxwell software, is discussed in [7]. The calculation methods to predict power loss, equivalent circuit values, and stray fields are presented. The simulation results are compared to the measured stray field of the inductive energy transfer system.

FEM modeling, design methodology, and the simulation results, applied to the development of a wireless energy transmission system, are shown in [8]. From the FEM simulations, it was obtained the magnetic field, the self-inductance, and the mutual inductance of the designed WET system.

In [9], the process of designing the coils of a WET system with FEM analysis and with MATLAB simulation, is presented. The experimental results are presented to verify the validity and reasonability of the design method.

In [10], a wireless power transfer system with series-parallel topology is analyzed and implemented. By the simulation it was proved that the electromagnetic field can be suppressed dramatically using a specific shield.

In [11], the finite element analysis method is used to investigate the magnetic field leakage from parallel WET systems. The effects of the magnetic flux leakage on the human body, i.e. by inducing electric field and voltage and the specific absorption rate (SAR) of the human body tissue are also simulated and evaluated.

The two-coil coupling of an inductive WET system for battery charging of an electric city-car is presented in [12]. The inductive parameters as a function of the coil distance and axial misalignment and the nearby electromagnetic field are investigated using a FEM analysis. The verification of the electromagnetic field admissibility for the humans is also performed. Finally, the design of the inductive parameters and the nearby electromagnetic fields are validated by measurements executed on the setup.

In [13], the magnetic field from the WET system is modeled and simulated considering a realistic vehicle, at a power level of 7 kW, using the Ansys Maxwell software. To validate the model, the simulated magnetic field is compared to the measured, maintaining the RMSE between the values 0.72 and 0.86. Finally, the electric field induced in a human body model by a leaked magnetic field from a WET system, was evaluated.

In this paper, the modeling and simulation of the wireless energy transfer system operating at frequencies of several kHz, are presented. The results of electric field (E-field) simulation are compared to the measurements of the electromagnetic emissions radiated by a realistic prototype of wireless energy transfer system.

In most of the earlier research works on the WET system, more attention is dedicated to the magnetic field (B-field) both as a computational model and as the simulation results. There are few research works dedicated to simulating and measuring of E-field. However, the coupling mechanisms of the electric and magnetic incident-field components are different. Thus, both must be determined separately to fully characterize the human exposure [14]. Moreover, the transmitter and receiver coils impedances increase with frequency. So, the E-field contribution may become dominant for the exposure (rather than the magnetic field) at frequencies above about 100 kHz [14]. Thus, the E-field simulating and measuring becomes important for the human exposure overall characterization. This research seeks to fill this gap by investigating the electric field produced by WET system, and, subsequently, the human exposure to that. So, this paper is a contribution in the field of EMC in the wireless energy transfer systems.

The rest of the paper is organized as follows: Section 2 presents the electromagnetic modeling, taking into consideration the Maxwell's equations as a basis. Section 3 presents the proposed design and simulation results of the WET charging system. Section 4 presents the experimental setup, taking into consideration the real prototype and the measurements of the electric field. Section 5 presents the discussion of the results. Section 6 presents the concluding remarks.

2. Modeling

2.1. Electric modeling

The schematic representation of a WET system is shown in Figure 2.

The equivalent circuit of the WET system is shown in Figure 3.

Figure 3 shows the equivalent circuit model of the 2-coils WET system using magnetically coupled resonators with self-inductances L_1 and L_2 , mutual inductance L_M , and copper losses R_1 and R_2 . Both coils are connected to the resonant capacitors C_1 and C_2 . R_S is the source resistance, R_L is the load resistance of the output.

The two coils are connected via a magnetic field, characterized by a coupling coefficient that is given by:

$$k_{12} = \frac{L_M}{\sqrt{L_1 L_2}} \tag{1}$$

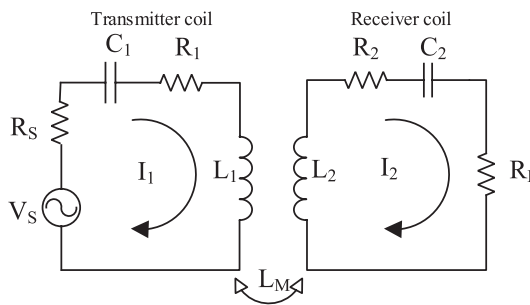


Figure 2. Schematic representation of a WET system.

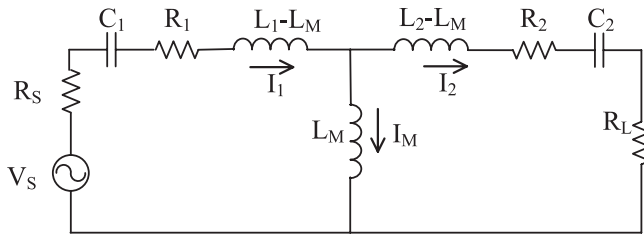


Figure 3. Equivalent circuit model of two-coil WET system.

The quality factor of the coils at resonance frequency ω_0 is given by:

$$Q = \frac{\omega_0 L}{R} \quad (2)$$

The two-coil model shown in Figure 3 can be analyzed using Kirchhoff's current/voltage laws, which are given by:

$$\left(R_S + R_1 + j\omega L_1 + \frac{1}{j\omega C_1} \right) I_1 - j\omega L_M I_2 = V_S \quad (3)$$

$$\left(R_L + R_2 + j\omega L_2 + \frac{1}{j\omega C_2} \right) I_2 - j\omega L_M I_1 = 0 \quad (4)$$

$$I_M = I_1 - I_2 \quad (5)$$

The loop impedances for the two coils are given by:

$$Z_1 = R_L + R_1 + j\omega L_1 + \frac{1}{j\omega C_1} \quad (6)$$

$$Z_2 = R_L + R_2 + j\omega L_2 + \frac{1}{j\omega C_2} \quad (7)$$

The transmitter and receiver side currents are given by:

$$I_1 = \frac{Z_2 V_S}{Z_1 Z_2 + \omega^2 L_M^2} \quad (8)$$

$$I_2 = \frac{j\omega L_M V_S}{Z_1 Z_2 + \omega^2 L_M^2} \quad (9)$$

At the resonance condition the reactive part of the impedance of the coils becomes zero. Therefore, at the resonant frequency the currents I_1 and I_2 can be simplified and given by:

$$I_1 = \frac{R'_2 V_S}{R'_1 R'_2 + \omega^2 L_M^2} \tag{10}$$

$$I_2 = \frac{j\omega L_M V_S}{R'_1 R'_2 + \omega^2 L_M^2} \tag{11}$$

where R'_1 and R'_2 , respectively are the total transmitting and receiving circuit resistances, are given by:

$$R'_1 = R_S + R_1 \tag{12}$$

$$R'_2 = R_2 + R_L \tag{13}$$

The power of the input side P_{in} and output power delivered to the load P_{out} is given by:

$$P_{in} = V_S I_1 \cos \phi \tag{14}$$

$$P_{out} = R_L I_2^2 = \frac{R_L \omega^2 L_M^2 V_S^2}{(R'_1 R'_2 + \omega^2 L_M^2)^2} \tag{15}$$

The overall power transfer efficiency can be given by:

$$\eta = \frac{P_{out}}{P_{in}} = \frac{R_L \omega^2 L_M^2}{R'_2 (R'_1 R'_2 + \omega^2 L_M^2) \cos \phi} \tag{16}$$

From (16), it can be seen that the power transfer efficiency is a function of the circuit parameters. The efficiency decreases quickly when drift apart from its resonant operating frequency. The high quality factor of transmitter and receiver coils is of crucial importance for the WET system efficiency at resonance frequency [15].

2.2. Magnetic modeling

The finite element method for frequency-domain analysis is used for the electromagnetic field simulation.

Most methods of computational electromagnetics are based on the differential form of the Maxwell's equations [16]. Adopted as a fundament, the Maxwell's equations describe all the classical electromagnetic phenomena, e.g. the Faraday's low of induction which is given by:

$$\nabla \times \mathbf{E} = -\frac{\partial \mathbf{B}}{\partial t} \tag{17}$$

The Ampere's law is given by:

$$\nabla \times \mathbf{H} = \mathbf{J} + \frac{\partial \mathbf{D}}{\partial t} \quad (18)$$

The Gauss' law for the electric field is given by:

$$\nabla \cdot \mathbf{D} = \rho \quad (19)$$

The Gauss' law for the magnetic field is given by:

$$\nabla \cdot \mathbf{B} = 0 \quad (20)$$

The density of the conductive currents may include both source currents and eddy currents [16].

In addition, a fundamental equation, which is known as the equation of continuity, is given by:

$$\nabla \cdot \mathbf{J} = -\frac{\partial \rho}{\partial t} \quad (21)$$

The field vectors \mathbf{E} , \mathbf{H} , \mathbf{D} , \mathbf{B} and \mathbf{J} are coupled with the environment via the relations [16] and are given by:

$$\mathbf{B} = \mu_0 \mu_r \mathbf{H} \quad \mathbf{D} = \varepsilon_0 \varepsilon_r \mathbf{E} \quad \mathbf{J} = \sigma \mathbf{E} \quad (22)$$

From (1) to (6) the magnetic vector potential \mathbf{A} is given by:

$$(j\omega\sigma - \omega^2 \varepsilon_0 \varepsilon_r) \mathbf{A} + \nabla \times \mathbf{H} = \mathbf{J} \quad (23)$$

The magnetic flux density \mathbf{B} can be written in terms of the magnetic vector potential \mathbf{A} , what allows to calculate the magnetic field distribution [16], given by:

$$\mathbf{B} = \nabla \times \mathbf{A} \quad (24)$$

In the end, the electric field is obtained using the Ampere's law (18).

3. Proposed design and simulation

3.1. Proposed design

The model of the WET system, including coils, ferrite core, and surrounding (air) domain, is simulated for the given setup and dimensions as in Section 4. The model size is in mm, used for the EM simulation, is shown in Figure 4.

The WET charger system consists of ferrite cores, with transmitter and receiver coils made of copper tube of radius $r = 3$ mm and the number of turns is $N = 5$, as it is shown further, in Figure 9. The air gap between the coils was varied in the range from 4 to 15 cm.

A frequency domain study was used to investigate the WET model, applying frequency, varying around the system's resonant frequency. For the WET electromagnetic field simulation system, which consists of two spiral coils with ferrite core, the 2D axisymmetric task was used. However, the spiral coils model is not axisymmetric. A common geometrical simplification consists in representation of the flat spiral inductor as a series of concentric loops,

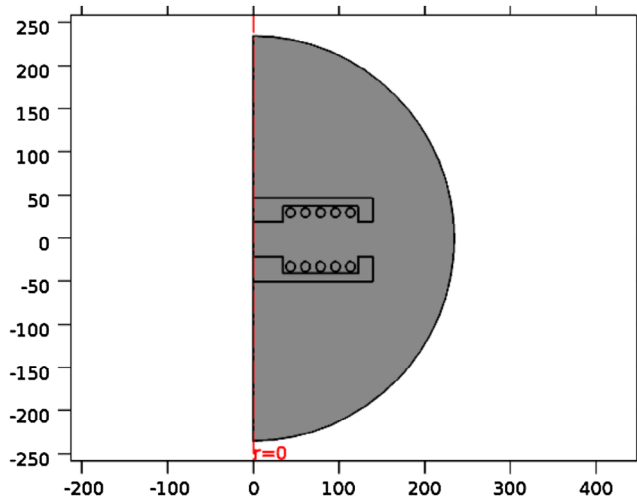


Figure 4. Modeling set of ferrite magnetic cores and inductive coils.

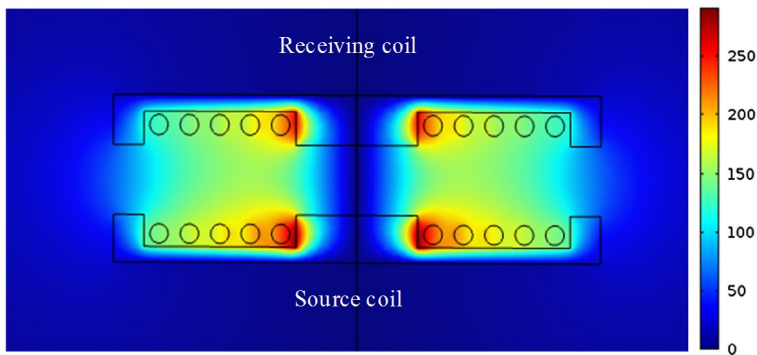


Figure 5. Electric field generated by WET system.

reducing that way the 3D problem to a 2D axisymmetric problem [17–19]. So, the model of coils was adapted for solving by 2D axisymmetric task, considering that the length of wire is practically the same for axisymmetric and non-axisymmetric model. Thus, it can be assumed that the accuracy of the solution is influenced negligibly.

3.2. Simulation results

The distribution intensities of the E-field and the B-field for distance up to 0.4 m in free space have been computed applying the FEM analysis and using numerical software.

The simulated magnitudes of the electric and magnetic fields from 800 W WET system were performed for the air gap between the source and the receiving coils of 4 cm. The electric field distribution for 142 kHz frequency range is shown in the Figure 5. The bar on the right is illustrating the values of Electric Field (V/m) in certain parts of the model.

Next, a variation of distance between the transmitting and the receiving coils was simulated. In Figure 6, the simulation results of the electric field \mathbf{E} distribution for the modeled

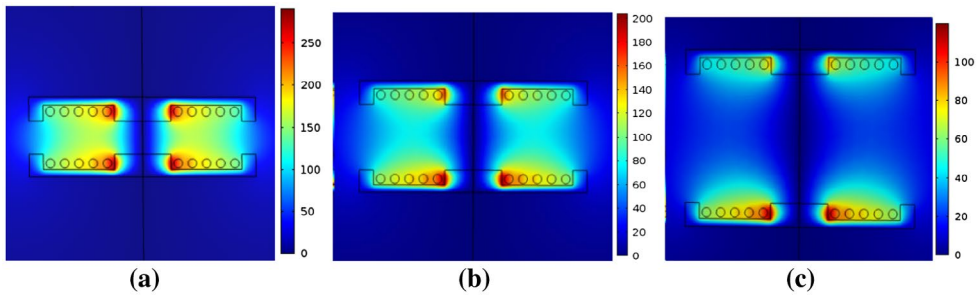


Figure 6. WET system E-field generated at air gap of: (a) 4 cm; (b) 8 cm; (c) 15 cm.

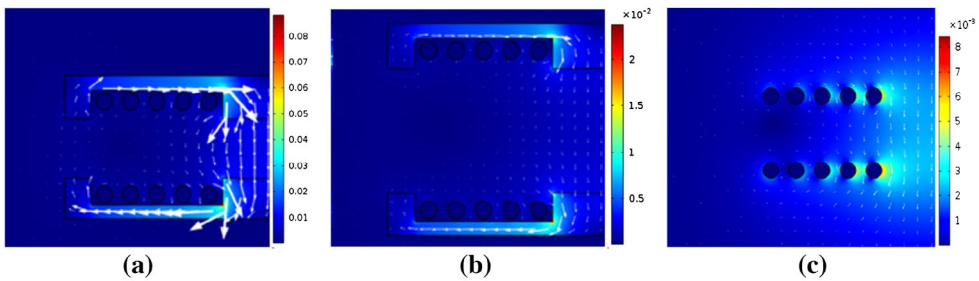


Figure 7. WET system B-field generated at air gap of: (a) 4 cm; (b) 8 cm; (c) 4 cm without ferrite cores.

WET charging system for air gap of 4 cm (a), 8 cm (b), and 15 cm (c) between the source and the receiving coils, are shown.

As it is shown in Figure 6, the field intensity exceeds the ICNIRP reference level in the regions limited by the ferrite cores. Outside these regions the field intensity is lower and it is below the exposure limits defined by ICNIRP [4]. These results also confirm that the strength of the electric field is decreasing with the increase of the distance.

In Figure 7, the magnetic flux density distribution for air gap of 4 cm (a) and 8 cm (b) between the source and the receiving coils with ferrite cores and for air gap of 4 cm without ferrite cores (c) is shown. The bar on the right illustrates the values of magnetic flux density B (T). The white arrows represent the magnitude and direction of the magnetic flux density vectors.

Figure 7 shows that the magnetic flux density is higher in the immediate vicinity of the ferrite cores and the coils, while away from the ferrites and coils, the magnetic field decreases rapidly. Hence, the magnetic flux density is higher at points where the coil is opposed to the ferrite core. It varies between 0.086 T for an air gap of 4 cm, 0.024 T for the air gap of 8 cm, and 0.008 T when the air gap is 4 cm, but without ferrite cores.

In addition, it is necessary to mention the function of the ferrite cores as efficient shields which allow to reduce stray magnetic fields produced by WET system. Ferromagnetic cores with high relative permeability is confining and guiding the magnetic flux. Thus, the distribution of electromagnetic field is limited to a region between the source and the receiver coils. So, the simulation was important to investigate the case without ferrite cores. The distribution of the electric field for WET system for air gap of 4 cm with and without ferrite cores, (a) and (b), respectively, is shown in the Figure 8.

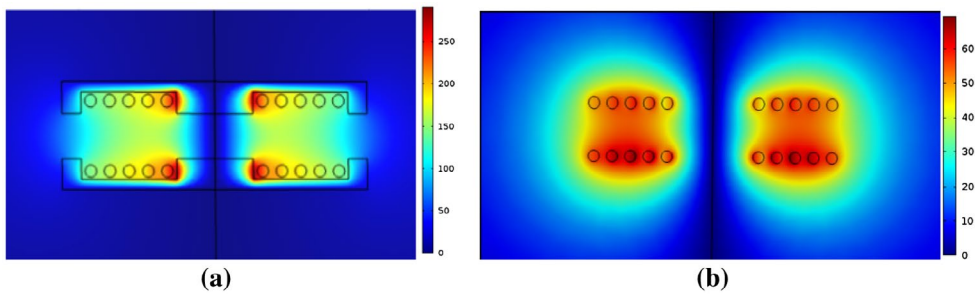


Figure 8. E-field distribution with (a) and without ferrite cores (b).

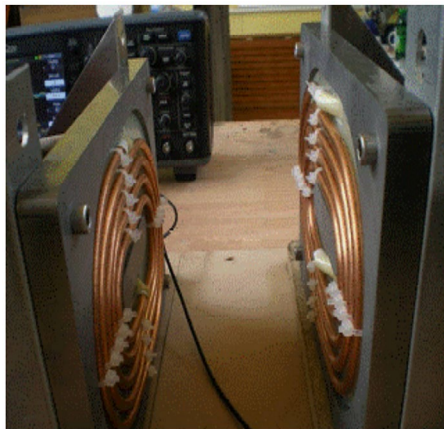


Figure 9. WET charger system.

In Figure 8(a), it can be observed that the electric field generated by WET system with ferrite cores, is more concentrated between ferrite plates than in Figure 8(b), without ferrite cores. Moreover, the dispersion of electric field is much limited in Figure 8(a). On the other hand, the electric field intensity generated by WET charger system is significantly higher when ferrite cores are applied, as it can be verified from the bar on the right sides of the figures. Thus, the ferrite cores make easier the electromagnetic field transfer, due to their lower reluctance, which enhances the energy transmitting, and concentrates the electromagnetic field between the plates, protecting the biological objects, as well.

The values of the E-field were determined at radial distances of 4, 20 and 40 cm from WET system, as in the case of measured practical values of the electric field, and are presented in the Table 1.

4. Experimental setup

4.1. Prototype

The model with the given setup and specifications was used for an experimental verification of the results of a previous research [3,20,22]. The WET system for EV charging is shown in the Figure 9.

The WET charger system for the transmission of 5 kW of output power is mounted at the Power Supply Electronics Laboratory of the Technical University of Sofia and the measurements are conducted at this laboratory. The prototype of the WET charger consists of:

- AC Rectifier and HF inverter, $P_{\max} = 5$ kW, frequency from 30 to 200 kHz;
- Ferrite core system of Transmitter and Receiver at a distance from 4 to 15 cm;
- HF Rectifier;
- DC charger, 20 V-180 V, 2 A-20 A with current control;
- Load resistors (RL) between 30 and 150 Ω ;
- A set of Li-Ion batteries, 10 Ah, 36 V.

The specific parameters of the coils are: transmitter coil, $L_1 = 64$ μH , $R_1 = 0.276$ Ω , $Q_1 = 206$; receiver coil, $L_2 = 30$ μH , $R_2 = 0.184$ Ω , $Q_2 = 145$.

The select distance between the transmitter and receiver coils and the operation frequency corresponds to the normal operation in charging batteries of electric vehicles.

The block diagram of studied WET system for EV charging is shown in Figure 10.

The set of the transmitting and the receiving coils was built on ferrite plates (Ferrites EE6527), with a copper tube spiral as in Figure 9, and later replaced by air cooled large section Litz wire to decrease the resistance of the coils and to reduce the skin effect at 142 kHz, that is corresponding to resonant frequency of the coils and capacitors set. The circuit parameters of the WET system are listed in Table 1. The ferrite cores have shown their advantage as magnetic shields against stray magnetic fields [21], protecting the human health. To reduce further the stray magnetic field, the ferrite material is combined with other shielding methods [10,21,22].

4.2. Prototype results

The objective of this experiment is the measuring of electromagnetic field levels emitted at different radial distances by the WET system for EV charging operating at 142 kHz frequency range.

To determine the level of E-field for different frequencies, a measuring instrument Narda SRM-3000 Selective Radiation Meter and an antenna for the 100 kHz/3 GHz frequency domain, was used. The RMS values of 20 first harmonics were measured, as they were generated by the WET system operating at frequency 142 kHz, an output power value of 228 W. The air gap between the transmitting and the receiving coils is 0.08 m and measurement distance value was 4, 20 and 40 cm, as shown in Figure 11.

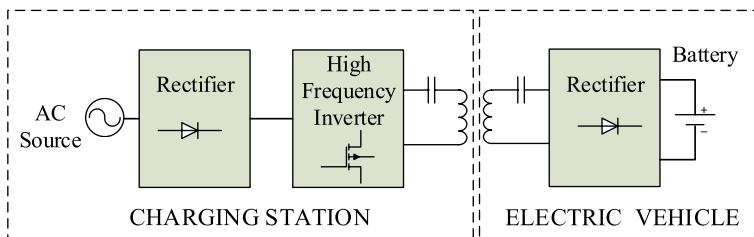


Figure 10. Main blocks of the WET system for EV charging.

Table 1. System parameters.

Parameter	Designation	Value
L_1	Transmitter side self-inductance	64 μH
L_2	Receiver side self-inductance	30 μH
$N_1 = N_2$	Number of turns in transmitter and receiver coils	5
C_1	Transmitter side capacitance	19.6 nF
C_2	Receiver side capacitance	41.9 nF
R_L	Load resistance	32 Ω
f_{res}	Resonant frequency	142 kHz

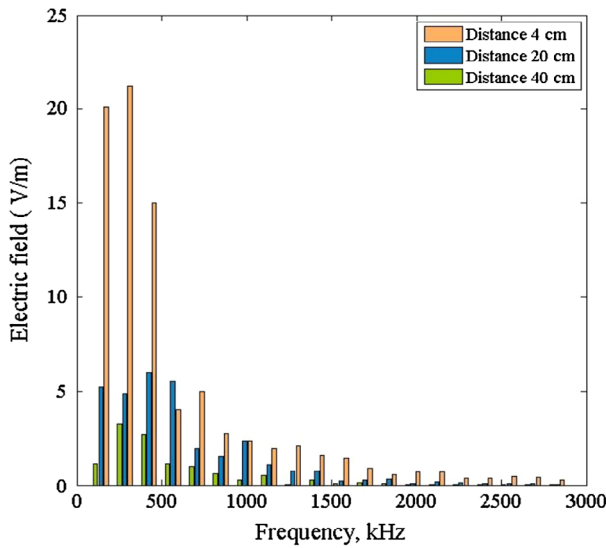


Figure 11. RMS values of the E-field harmonics generated by the WET system with air gap of 8 cm.

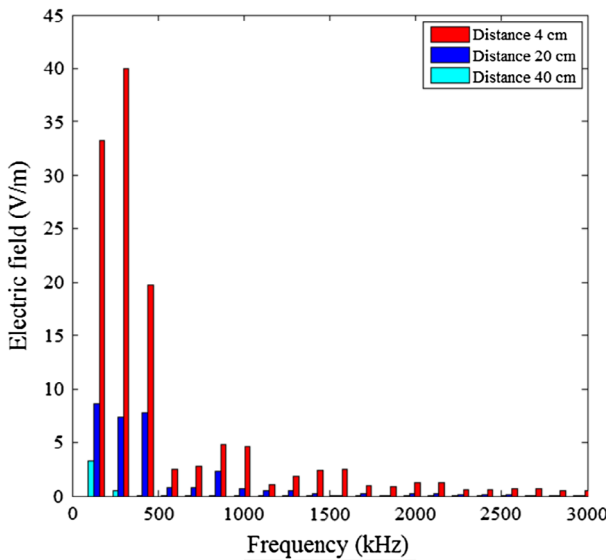


Figure 12. RMS values of the E-field harmonics generated by the WET system with air gap of 4 cm.

The measurements of E-field were performed also for the output power value of the 800 W at the same measurement distances. The RMS values of 20 first harmonics generated by WET system operating at frequency value of 142 kHz, at output power of 800 W. The air gap is 0.04 m and the measurement is done at distance values of the 4, 20 or 40 cm, as shown in Figure 12.

Figures 11 and 12 show that for the measurement distance value of the 4 cm the predominant harmonic is the 2nd. For the measurement distance value of 20 cm the predominant harmonics are the 1st and the 3rd. Comparing the power levels, it can be seen that for the output power 228 W, the 3rd harmonic is higher than the 1st one, and for the output power value of the 800 W the 1st harmonic is slightly higher than the 3rd one. For the measurement distance value of the 40 cm and the output power value of the 228 W the predominant harmonics are the 2nd and 3rd, but for the output power value of the 800 W the predominant harmonic is the 1st.

Through an evaluation of the results obtained at the studied WET system, it is possible to confirm that the produced maximum value of the E-field for the output power value of the 800 W at the distance of 0.04 m is more than twice lower than the safety limits for general public defined by the ICNIRP, i.e. is 40.5 V/m for 2nd harmonic. The RMS values of E-field for the 1st harmonic in function of the measurement distance and transferred power values of the 120, 300, or 800 W [3] is shown in Figure 13.

Figure 13 shows that for the frequency value of the 142 kHz, the slope of the E-field curves is larger between the distances of 4 and 20 cm, while it is less for the distances between the 20 and 100 cm.

5. Discussing of the results

In Table 2, the measured and simulated magnitudes of the electric field from the studied WET system are compared.

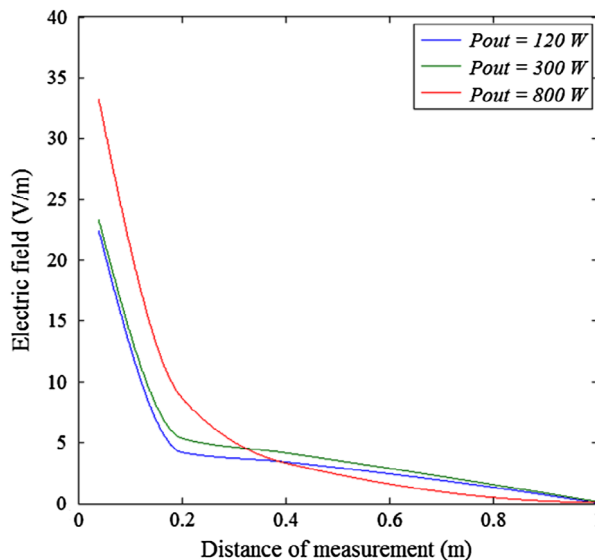


Figure 13. E-field 1st harmonic generated by WET system.

Table 2. Electric field strength.

Distance of measurement (cm)	Air gap of 4 cm			Air gap of 8 cm		
	Pout = 800 W			Pout = 228 W		
	Electric Field (1st harmonic), V/m					
	Simulated	Measured	Difference	Simulated	Measured	Difference
4	31.02	33.19	6.54%	18.79	20.11	6.56%
20	7.98	8.65	7.75%	4.79	5.22	8.24%
40	3.08	3.32	7.2%	1.05	1.15	8.7%

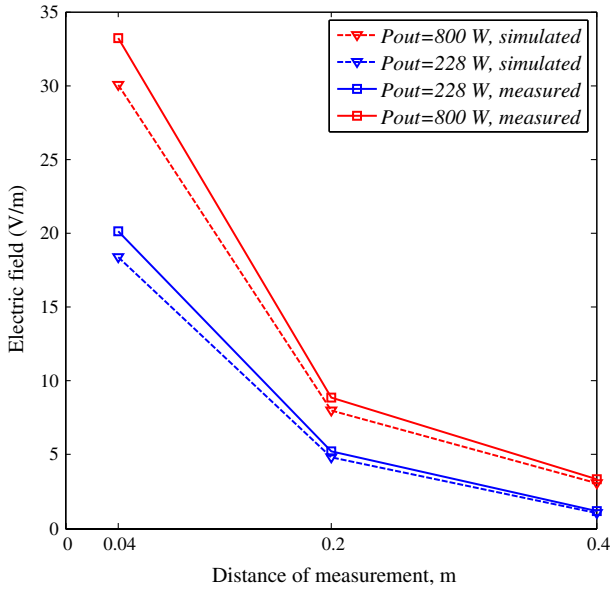


Figure 14. Simulated and measured results of E-field 1st harmonic generated by WET system.

Table 3. Simulations root mean square error (RMSE).

Simulation	Pout = 228 W	Pout = 800 W
RMSE	0.8036 V/m	1.3185 V/m

The results show that the measured and simulated electric field values have good correlation in all cases revealing a simulation error of 8.7%. The simulated and measured results of E-field 1st harmonic generated by WET system is shown in Figure 14.

In order to evaluate the accuracy of the model a Root Mean Square Error (RMSE) was calculated. The RMSE is given by:

$$RMSE = \sqrt{\frac{\sum_{i=1}^n (E_{Si} - E_{Mi})^2}{n}} \tag{9}$$

where n is the number of data, E_{Si} is the i -th simulated E-field, E_{Mi} is i -th measured E-field. The simulations RMSE for the E-field 1st harmonic versus distance of measurement curves is shown in Table 3.

The simulation results for the electric field distribution in the studied WET system are in a good agreement with the measurement data. However, the simulation results are in general, lower than measured results. This discrepancy between simulated and measured results can be explained by the simplification of coil model. The transmitter and receiver coils have spiral topology, however, the coil model is not exact spiral geometry, and it must be adapted for solving in 2D axisymmetric space dimension. The approach when the spiral coil is modeled as a set of circular filamentary currents is frequently used in computational simulation practice. Moreover, the WPT system considered in this research, in fact is not a linear system. The error between the simulation result and the experimental result can also be explained by the linearity assumptions taken in the computational simulation.

From the results, the following observations are done:

- from the simulation results it is observed that a strong E-field is present in a close proximity to the ferrite core and the transmitting coil;
- as it shown in Figures 6–8, the regions where the electric field intensity exceeds the reference level defined by ICNIRP Guidelines [2] are limited by the ferrite cores.
- the maximum value of electric field registered in the above-mentioned area, for the output power of the 800 W, is 225 V/m. However, outside the ferrite regions, the E-field intensity is below the exposure limits defined by ICNIRP [3]. That is, the EMF intensity is limited to 40.5 V/m at 284 kHz of frequency, i.e. 2nd harmonic and at 4 cm distance, as in Figure 12;
- the practically measured values of the electric field, are a function of the distance to the measuring antenna from the WET system, as expected and described in Figure 13;
- the electric field is much stronger directly next to the WET system, but decreases significantly with the distance, as expected;
- the ferrite cores have an important function in the WET system of confining and guiding the magnetic flux.

6. Conclusions

In this study, the modeling and simulation of the WET system operating at the frequency of 142 kHz is performed. First, the electric field and the magnetic flux density for different air gap sizes between the transmitter and the receiver was simulated computationally, considering the given setup and specifications. Then measurements of the electric field, produced by the WET system for EV charging, were performed. Finally, the simulated electric field was compared to the measured values to confirm the validity of the finite element model. The results are presented and compared to the measurements of the electromagnetic emissions radiated by the prototype of WET system. The comparison between the obtained experimental values of the electric field E and the simulation results shows a simulation error of roughly 8.7%.

Nomenclature

Vectors

A	magnetic vector potential
E	electric field intensity
H	magnetic field intensity
D	electric flux density
B	magnetic flux density
J	electric current density

Constants or variables

ρ	volume charge density
σ	electrical conductivity
ϵ_0	permittivity of free space
ϵ_r	relative permittivity of a material
μ_0	permeability of free space
μ_r	relative permeability of a material
ω	angular frequency
V_s	AC power source
R_s	source resistance
R_1	transmitter coil resistance
L_1	transmitter coil inductance
C_1	transmitter side capacitance
L_M	mutual inductance between the transmitter and the receiver coils
R_2	receiver coil resistance
L_2	receiver coil inductance
C_2	receiver side capacitance
R_L	load resistance
k_{12}	coupling coefficient
Q_1	quality factor of transmitter coil
Q_2	quality factor of receiver coil
I_1	transmitter side current
I_2	receiver side current
R'_2	total transmitting circuit resistances
R'_2	total receiving circuit resistances
P_{in}	power of the input side
P_{out}	power of the output side
$\cos\varphi$	power factor
η	power transfer efficiency

Disclosure statement

No potential conflict of interest was reported by the authors.

Funding

This work is funded by Portuguese Funds through the Foundation for Science and Technology-FCT under the project LAETA 2015-2020, reference UID/EMS/50022/2013.

ORCID

R. Melicio  <http://orcid.org/0000-0002-1081-2729>

V. Fernão Pires  <http://orcid.org/0000-0002-3764-0955>

References

- [1] Kalialakis C, Carvalho NC, Shinohara N, et al. Selected developments in wireless power transfer standards and regulations. *IEEE Communications Magazine*; 2016 Jul; p. 9–11.
- [2] Pinto R, Lopresto V, Genovese A. Human exposure to wireless power transfer systems: a numerical dosimetric study. In: *Proceedings of 11th European Conference on Antennas and Propagation (EUCAP)*; Paris, France; 2017 Mar. p. 1–3.
- [3] Baikova E, Valtchev S, Melicio R, et al. Study of the electromagnetic interference generated by wireless power transfer systems. *Int Rev Electr Eng*. 2016 Nov;11(5):526–534.
- [4] International Commission on Non-Ionizing Radiation Protection (ICNIRP), Guidelines for limiting exposure to time-varying electric, magnetic and electromagnetic fields (up to 300 GHz. *Health Phys*. 1998;74:494–522.
- [5] Agarwal A, Gupta A, Sen D. Wireless power using magnetic conductor. *Int Adv Res J Sci Eng Technol*. 2015 May;2(1):217–220.
- [6] Isaev YN, Vasileva OV, Budko AA, et al. Parameters assessment of the inductively-coupled circuit for wireless power transfer. In: *Proceedings of International Conference on Mechanical Engineering, Automation and Control Systems*; Moscow, Russia; 2016 May. p. 1–6.
- [7] Bosshard R, Kolar JW, Wunsch B. Accurate finite-element modeling and experimental verification of inductive power transfer coil design. In: *Proceedings of 29th Annual IEEE Applied Power Electronics Conference and Exposition (APEC)*; Fort Worth (TX); 2014 Mar. p. 1648–1653.
- [8] Jorgetto MFC, Guilherme de e Melo A, Canesin CA. Wireless inductive power transfer, oriented modeling and design. In: *Proceedings of IEEE 13th Brazilian Power Electronics Conference and 1st Southern Power Electronics Conference (COBEP/SPEC)*; Ceará, Brazil; 2015 Nov–Dec. p. 1–6.
- [9] Chang R, Quan L, Zhu X, et al. Design of a wireless power transfer system for EV application based on finite element analysis and MATLAB simulation. In: *Proceedings of IEEE Conference and Expo Transportation Electrification Asia-Pacific (ITEC Asia-Pacific)*; Beijing, China; 2014 Aug–Sep. p. 1–4.
- [10] Kim S, Park H-H, Kim J, et al. Design and analysis of a resonant reactive shield for a wireless power electric vehicle. *IEEE Trans Microw Theory Tech*. 2014 Apr;62(4):1057–1066.
- [11] Wen F, Huang X. Human exposure to electromagnetic fields from parallel wireless power transfer systems. *Int J Environ Res Public Health*. 2017 Feb;14(2):1–15.
- [12] Mude KN, Bertoluzzo M, Buja G, et al. Design and experimentation of two-coil coupling for electric city-car WPT charging. *J Electromagn Waves Appl*. 2016 Nov;30(1):70–88.
- [13] Laakso I, Hirata A. Evaluation of the induced electric field and compliance procedure for a wireless power transfer system in an electrical vehicle. *Phys Med Biol*. 2013 Nov;58(21):7583–7593.
- [14] International Agency for Research on Cancer (IARC). Non-ionizing radiation, part 2: radiofrequency electromagnetic fields. *IARC Monograph*, vol. 102. Lyon, France; 2013.
- [15] Romba LF, Valtchev S, Melicio R. Three-phase magnetic field system for wireless energy transfer. In: *Proceedings of IEEE International Symposium on Power Electronics, Electrical Drives and Motion (SPEEDAM)*; Capri, Italy; 2016 Jun. p. 73–78.
- [16] Šolín P. *Partial differential equations and the finite element method*. Hoboken (NJ): Wiley; 2006. p. 269–291.
- [17] Ke L, Yan G, Yan S, et al. Improvement of the coupling factor of Litz-wire coil pair with ferrite substrate for transcutaneous energy transfer system. *Prog Electromagn Res M*. 2014;39:41–52.

- [18] Rueter D. Induction coil as a non-contacting ultrasound transmitter and detector: modeling of magnetic fields for improving the performance. *Ultrasonics*. 2016 Feb;65:200–210.
- [19] Gendron M, Hazel B, Boudreault E, et al. Modeling circular inductors coupled to a semi-infinite magnetic medium considering the proximity effect. *J Electromagn Waves Appl*. 2017;31(13):1232–1254.
- [20] Baikova E, Valtchev S, Melicio R, et al. Study on electromagnetic emissions from wireless energy transfer. In: *Proceedings of IEEE International Power Electronics and Motion Control Conference (PEMC)*; Varna, Bulgaria; 2016 Sept. p. 492–497.
- [21] Strauch L, Pavlin M, Bregar VB. Optimization, design, and modeling of ferrite core geometry for inductive wireless power transfer. *Int J Appl Electromagn Mech*. 2015 Sept;49(1):145–155.
- [22] Gigov G, Krusteva A, Valtchev S. Experimental study of wireless inductive system for electric vehicles batteries charging. In: *Proceedings of IEEE International Power Electronics and Motion Control Conference (PEMC)*; Varna, Bulgaria; 2016 Sept. p. 286–290.